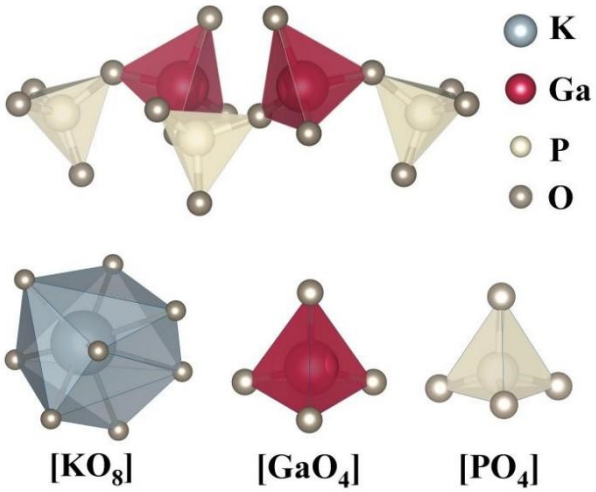

Figure S1. The coordination environment of cations.

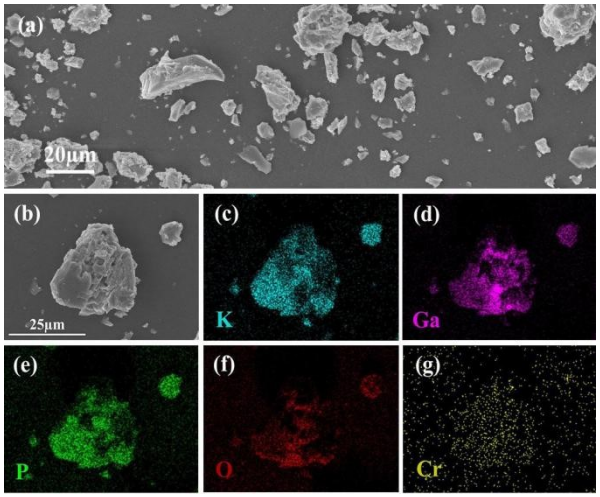

Figure S2. Scanning electron microscopy (SEM) image of $K_3Ga_{1.93}(PO_4)_3$:0.07Cr^{3+}, along with the corresponding elemental distribution mapping.

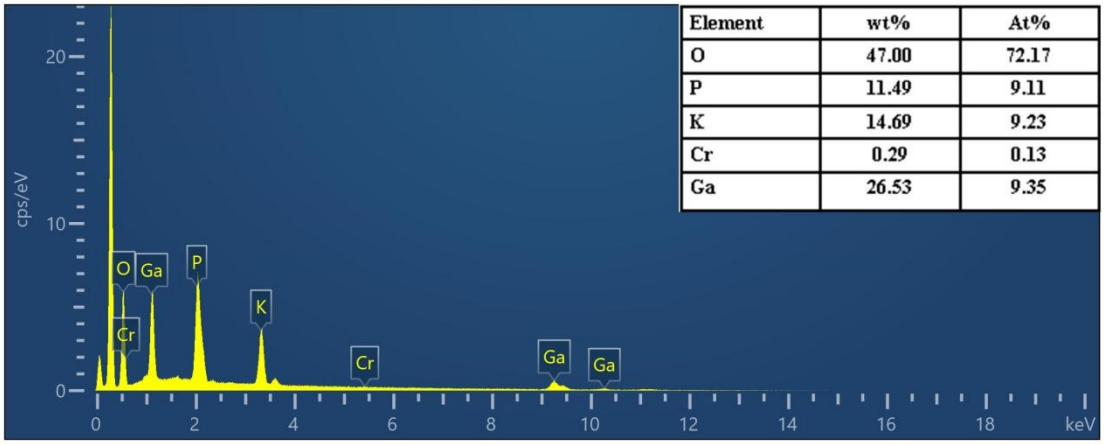

Element	wt%	At%
O	47.00	72.17
P	11.49	9.11
K	14.69	9.23
Cr	0.29	0.13
Ga	26.53	9.35

Figure S3. Stoichiometric ratios of various elements in the composite.

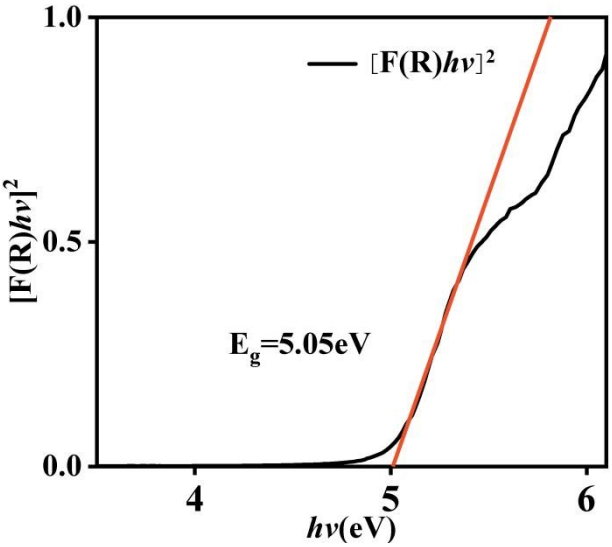

Figure S4. The optical band gap of KGP sample estimated based on Kubelka–Munk function.

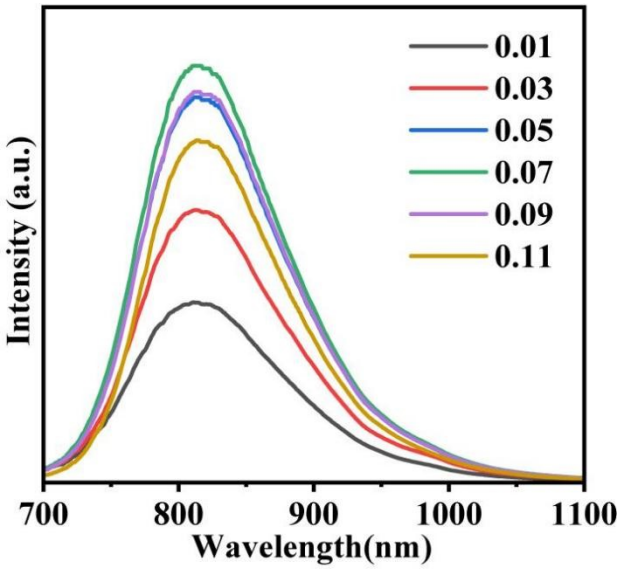

Figure S5. The Emission spectra of $K_3Ga_{2-x}(PO_4)_3$: xCr^{3+} (x = 0.01, 0.03, 0.05, 0.07, 0.9 and 0.11) samples excited by 452 nm.

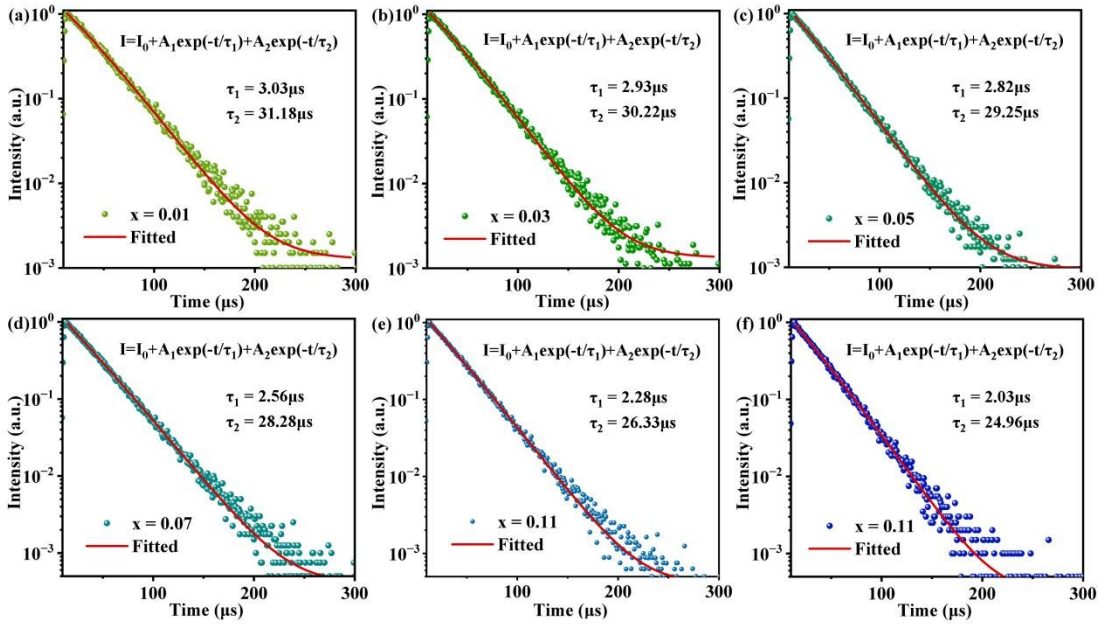

Figure S6. (a-f) Double-exponential fitted decay curves of $K_3Ga_{2-x}(PO_4)_3$: xCr^{3+} (x = 0.01, 0.03, 0.05, 0.07, 0.09 and 0.11) excited by 452 nm and monitored at 822 nm.

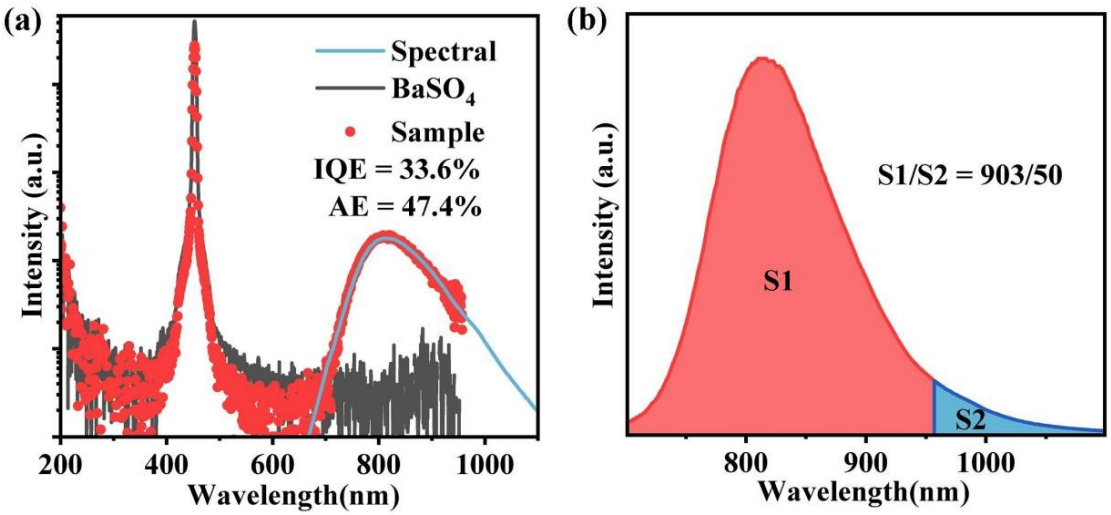

Figure S7. (a)Quantum yield measurement of the $K_3Ga_{1.93}Cr_{0.07}(PO_4)_3$ phosphor under 452 nm excitation; (b)The amplified emission spectra and the reference in 700 nm to 1100 nm region.

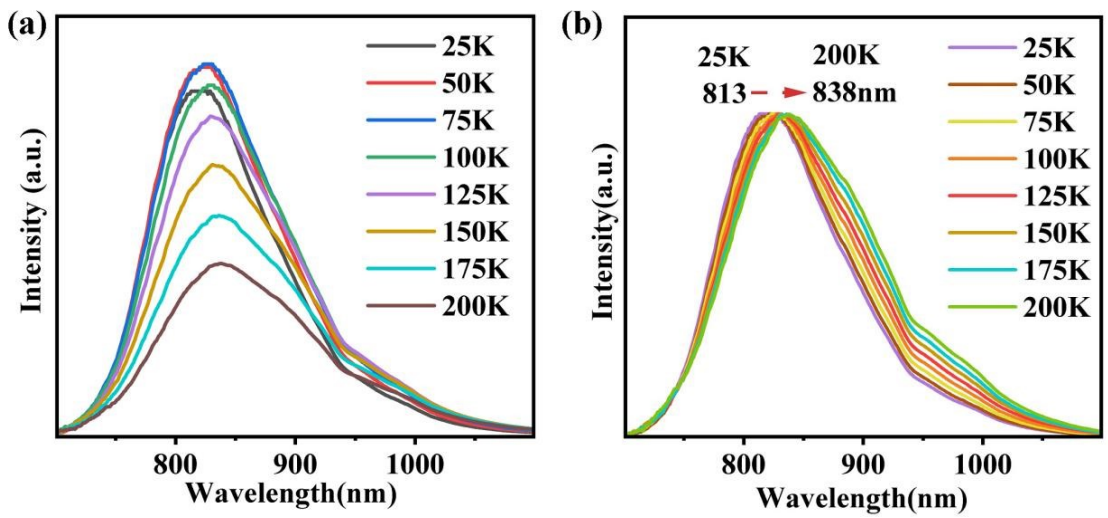

Figure S8. (a)Temperature-dependent emission spectra; (b) normalized results of $K_3Ga_{1.93}Cr_{0.07}(PO_4)_3$ under 452 nm excitation in temperature region of 298-473 K.

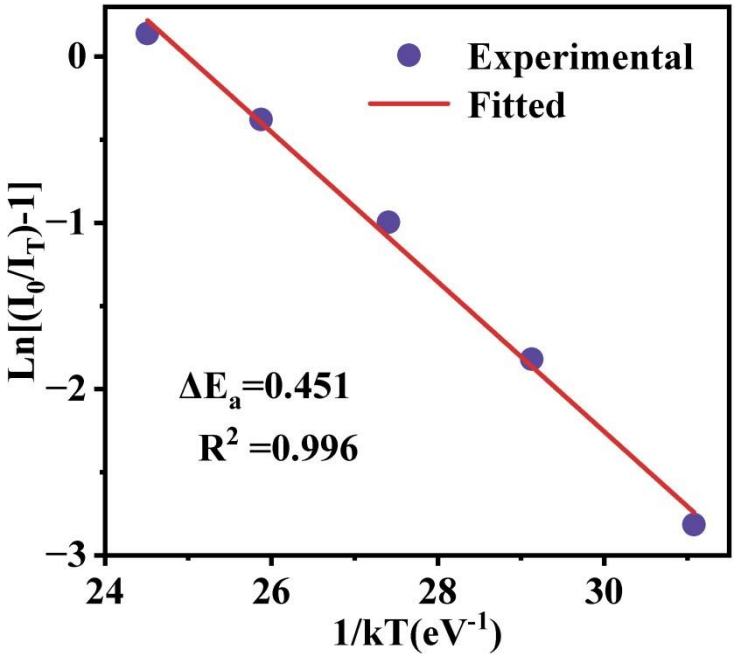

Figure S9. The linear relationship between $Ln(I_0/I_T\text{-}1)$ vs $1/kT$ and the fitted activation energy for thermal quenching.

Table S1. The refined atomic positions of $K_3Ga_2(PO_4)_3$.

Atom	*x*	*y*	*z*	Occ.	Uiso	Site
P(1)	0.15194	0.7152	1.28804	1	0.007	4a
P(2)	0.29802	0.8131	0.79667	1	0.009	4a
P(3)	0.26191	0.50328	0.86661	1	0.011	4a
K(1)	0.45271	0.6466	0.59513	1	0.013	4a
K(2)	0.00977	0.90013	1.12307	1	0.014	4a

K(3)	0.18095	0.51039	0.3947	1	0.021	4a
Ga(1)	0.13278	0.66831	0.94007	1	0.008	4a
Ga(2)	0.347	0.84139	1.42835	1	0.008	4a
O(1)	0.2085	0.801	1.2861	1	0.01	4a
O(2)	0.0312	0.7091	1.4225	1	0.013	4a
O(3)	0.2809	0.6573	1.3087	1	0.015	4a
O(4)	0.0625	0.7052	1.13	1	0.011	4a
O(5)	0.1859	0.8666	0.8761	1	0.023	4a
O(6)	0.2647	0.8088	0.6167	1	0.022	4a
O(7)	0.2904	0.7266	0.8591	1	0.016	4a
O(8)	0.4661	0.8404	0.8104	1	0.023	4a
O(9)	0.2189	0.5732	0.9791	1	0.014	4a
O(10)	0.4055	0.4651	0.9277	1	0.016	4a
O(11)	0.1208	0.4443	0.8917	1	0.017	4a
O(12)	0.2674	0.5301	0.6966	1	0.016	4a

Table S2. PL properties of several Cr^{3+}-doped NIR phosphors.

Host matrix	$\lambda_{em.}$(nm)	PLQY	fwhm	References
KGP	822	70.9	122	This work
$Na_3Al_2(PO_4)_2F_3$	815	54.4	157	[1]
$Li_2Sr_2Al(PO_4)_3$	823	61	178	[2]
La_2MgZrO_6	825	58	210	[3]
$GaMgGeO_3$	830	58.3	186	[4]
$Ga_{2-2x}Zn_xGe_xO_3$	808	41	190	[5]
$LiScO_2$	830	21	165	[6]

Table S3. The detailed parameters of device, including voltage, current, input power, output power of blue LED chip, NIR output power, and NIR conversion efficiency as function of current.

Current (mA)	Voltage (V)	input power (mW)	output power of blue light part(mW)	output power of NIR part(mW)	NIR photoelectric conversion efficiency (%)
20	2.605	52	0.239	3.139	6.04
40	2.651	105	0.49	6.097	5.81
59	2.687	159	0.75	9.424	5.93
80	2.72	216	0.991	12.082	5.59
100	2.748	274	1.236	14.845	5.42
120	2.776	333	1.455	16.68	5.01

160	2.828	453	1.946	21.965	4.85
200	2.878	575	2.394	26.037	4.53
240	2.93	703	2.895	29.989	4.27
280	2.971	831	3.291	34.004	4.09
320	3.02	966	3.772	37.579	3.89

References

(1) Wu, H. J.; Liang, S. S.; You, W. X.; Liu, L.; Guo, Y. W.; Wang, S. J.; Song, L. P.; Wang, Z. H.; Zhu, H. M. A broadband near-infrared emission Na3Al2(PO4)2F3: Cr3+ phosphor exhibiting zero photoluminescence quenching at 398 K. *J. Mater. Chem. C* **2024**, *12* (13), 4825-4834. DOI: 10.1039/d4tc00004h.

(2) Zhang, X. B.; Zhang, L.; Xu, Y. H.; Wu, X. D.; Yin, S. W.; Zhong, C. S.; You, H. P. Broadband Near-Infrared-Emitting Phosphors with Suppressed Concentration Quenching in a Two-Dimensional Structure. *Inorg. Chem.* **2022**, *61* (19), 7597-7607. DOI: 10.1021/acs.inorgchem.2c00778.

(3) Zeng, H. T.; Zhou, T. L.; Wang, L.; Xie, R. J. Two-Site Occupation for Exploring Ultra-Broadband Near-Infrared Phosphor-Double-Perovskite La2MgZrO6:Cr3+. *Chem. Mat.* **2019**, *31* (14), 5245-5253. DOI: 10.1021/acs.chemmater.9b01587.

(4) Zhong, J. Y.; Zeng, L. W.; Zhao, W. R.; Brgoch, J. Producing Tunable Broadband Near-Infrared Emission through Co- Substitution in (Ga1-xMgx)(Ga1-xGex)O3: Cr3+. *Acs Applied Materials & Interfaces* **2022**, *14* (45), 51157-51164. DOI: 10.1021/acsami.2c17902.

(5) Zeng, L. W.; Zhong, J. Y.; Lin, W. B.; Zhao, W. R. Achieving a tunable and ultra-broadband near-infrared emission in the Ga2-2xZnxGexO3: Cr3+ phosphor. *Dalton Trans.* **2022**, *51* (43), 16740-16747. DOI: 10.1039/d2dt02971e.

(6) Qin, Y. F.; Zhong, J. Y.; Du, F.; Wen, J.; Lin, Z. R.; Zhao, W. R. Tunable broadband near-infrared emission in LiScO2:Cr3+ phosphor induced by the variation of chromium ion concentration. *Journal of Luminescence* **2023**, *257*. DOI: 10.1016/j.jlumin.2023.119758.